Università degli Studi di Padova

Dipartimento di Pediatria

SCUOLA DI DOTTORATO DI RICERCA IN : MEDICINA DELLO SVILUPPO E SCIENZE DELLA PROGRAMMAZIONE

INDIRIZZO: GENETICA E BIOCHIMICA CLINICA

CICLO XXII

L-citrulline has a protective effect in hyperoxic lung damage and improves matrix remodeling and alveolarization

Direttore della Scuola : Ch.mo Prof. Giuseppe Basso

Coordinatore d'indirizzo: Ch.mo Prof. Maurizio Scarpa

Supervisore :Ch.mo Prof. Lino Chiandetti

Dottorando : Dott.ssa Michela Alfiero Bordigato

RIASSUNTO

Background

Nonostante i progressi tecnologici e terapeutici degli ultimi anni, la displasia broncopolmonare (BPD) rimane ancora causa principale di morbilità respiratoria nei neonati prematuri di peso molto basso (VLBW).

L'ossido nitrico (NO) e le metalloproteasi di matrice (MMP) hanno un ruolo cruciale nell'omeostasi della struttura e della matrice broncoalveolare.

In particolare, sempre maggiore è l'evidenza scientifica che attribuisce all'ossido nitrico endogeno un ruolo vitale nello sviluppo alveolare e vascolare del polmone immaturo.

Oltre ad essere un potente vasodilatatore, l'NO ha molti effetti biologici rilevanti: migliora lo scambio gassoso, ha azione antiinfiammatoria e antiossidante, stimola appunto l'angiogenesi e la crescita del polmone immaturo. Il potenziale ruolo di una terapia con NO inalatorio per la prevenzione della BPD è stato recente oggetto di vari studi, ma non è stato ancora chiaramente definito (Horst et al. Am J Physiol Lung Cell Mol Physiol, 2007; Lin et al, Pediatr Res, 2005; McCurnin et al, Am J Physiol Lung Cell Mol Physiol 2005).

L'arginina è il substrato dell'ossido nitrico sintetasi per la produzione di NO. Ci sono evidenze che la supplementazione con L-arginina aumenti la vasodilatazione endotelio-dipendente, mediata dall'NO (Bode-Boger et al, Vasc Med 2003; Piatti et al, Diabetes Care, 2001).

Dopo somministrazione orale però l'arginina è soggetta a un intenso metabolismo presistemico; è stato dimostrato che la supplementazione orale con L-citrullina aumenta significativamente le concentrazioni plasmatiche di arginina, in modo dose dipendente, più che la somministrazione di L-arginina stessa (Kuhn et al. Circulation 2002; Schwedhelm et al. Br J Clin Pharmacol, 2007). Infatti la citrullina viene convertita in arginina sia nelle cellule del tubulo renale prossimale, che in molte cellule in grado di produrre NO (cellule endoteliali e macrofagi), che utilizzano la citrullina come substrato per produrre arginina.

Obiettivi del progetto di ricerca

Scopo di questo progetto era valutare se la somministrazione di L-citrullina, aumentando i livelli plasmatici e/o tissutali di arginina e stimolando la produzione endogena di NO, potesse attenuare il danno polmonare indotto dall'iperossia in un modello sperimentale di BPD.

Materiali e metodi

Ratti neonati wild-type Sprague-Dawley (n=40) sono stati esposti a moderata iperossia moderata (FiO_2 60%) per i primi 14 giorni di vita (Man Yi, Am J Respir Crit Care Med, 2004): 12 non hanno ricevuto alcun trattamento, 18 sono stati trattati con L-citrullina 1g/kg/die intraperitoneale, 10 sono stati trattati quotidianamente con placebo (soluzione salina intraperitoneale). Un gruppo di ulteriori 10 ratti sono stati mantenuti in aria ambiente per i primi 14 giorni di vita e utilizzati come controlli. Tutte le procedure sugli animali sono state condotte in maniera conforme al D. L. 116/1992 e secondo autorizzazione n. 173/2006-B del 4.12.2006.

Per valutare l'effetto del trattamento è stata analizzata la morfometria su tessuto polmonare. Ulteriori marker di sviluppo polmonare sono stati analizzati, in particolare VEGF e metalloproteasi 2 (MMP2).

Risultati

Il numero di alveoli /mm^2 risultava più basso nei ratti esposti a iperossia e in quelli trattati con placebo rispetto ai ratti cresciuti in aria ambiente e a quelli trattati con L-citrullina ($p<0.05$).

I livelli sierici di arginina risultavano più elevati nel gruppo trattato con L-citrullina ($p<0.05$). Il trattamento con L-citrullina non modificava l'espressione del gene per la metalloproteasi2 (MMP2), ma la proteina attiva MMP2 risultava più elevata nel lavaggio broncoalveolare dei ratti trattati con L-citrullina ($p<0.05$). Nei ratti trattati con L-citrullina, inoltre, si evidenziava un incremento significativo dell'espressione del gene per il VEGF a livello polmonare ($p<0.05$).

Conclusioni

La somministrazione di L-citrullina sembra elevare i livelli plasmatici di arginina e potrebbe pertanto promuovere la produzione endogena di NO: il trattamento con citrullina sembra promettente per migliorare la crescita alveolare e il controllo della matrice nel danno polmonare indotto dall'iperossia.

Abstract

Even moderate hyperoxia alters alveolar and vascular lung morphogenesis. Nitric oxide (NO) and matrix metalloproteinases (MMP) have a crucial role in the homeostasis of the matrix and bronchoalveolar structure, and may be regulated abnormally by exposure to hyperoxia.

We hypothesize that L-citrulline, by raising the serum levels of L-arginine and enhancing endogenous NO synthesis, might attenuate hyperoxia-induced lung injury in an experimental model of bronchopulmonary dysplasia (BPD).

Neonatal rats (1 day old) were exposed to 60% oxygen or room air for 14 days and administered L-citrulline or a vehicle. Serum was tested for arginine level, which rose in the L-citrulline-treated group ($p<0.05$). Alveolar number decreased in the hyperoxia and vehicle-treated groups, when compared with the room air and L-citrulline treated group ($p<0.05$). L-citrulline did not affect matrix metalloproteinase2 (MMP2) gene expression, but MMP2 active protein resulted to be higher in bronchoalveolar lavage fluid of the citrulline-treated rats ($p<0.05$). At the same time, an increased lung VEGF gene expression ($p<0.05$) and protein immunostaining were also seen in the rats treated with L-citrulline. We conclude that: (i) the main effects of L-citrulline are an increased serum level of arginine, as a promoter and a substrate of the nitric oxide synthase; and (ii) a better alveolar growth and matrix control in hyperoxia-induced lung damage seems promising.

Introduction

Despite technological and therapeutic advances over the past several years, bronchopulmonary dysplasia (BPD) remains a leading cause of respiratory morbidity in very low birth weight infants.

Premature birth with injury to the immature lung disrupts the normal sequence of lung growth and leads to the development of severe chronic lung disease.

The term BPD was introduced in the 1960s by Northway et al(1).The histological findings in these patients showed severe injury to the large airways and focal fibrosis of lung parenchyma. The long-term outcomes of these patients were persistent pulmonary dysfunction. However, since the introduction of surfactant therapy and new ventilator strategies, the clinical course and outcomes of premature babies with respiratory distress syndrome have changed considerably(2). Moreover, the progress of neonatal care and the introduction of antenatal steroid therapy lowered the threshold for survival: now, infants with BPD are mainly premature newborns who are far less mature and with much lower birth weight than previously described. A uniform arrest in lung development with fewer alveoli, and aberrant microvasculature can be detected in extremely low gestational age preterm infants who develop BPD nowadays. The airways show little to no injury and no fibrosis is detected. For these reasons and shifts in patient population and history, the term ‘new BPD’ was introduced (3) and the clinical definition was revised.

More typically, infants with cronic lung disease now have less severe acute respiratory disease early, and, at autopsy, lung histology shows more uniform and milder regions of injury, with signs of impaired alveolar and vascular growth becoming more prominent (2).

The embryonic development of the lung is a well-defined sequence of proliferation and differentiation, which has been histologically characterized (4). The different phases of

gestational lung development are shown in Figure 1. The developing lung histologically resembles an exocrine gland during the pseudoglandular phase from 6 to 16 weeks. By 16 weeks, all major elements of the lung have formed except those involved in gas exchange: at this stage, respiration is therefore not possible. Because cranial segments of the lung develop faster than caudal ones, the canalicular phase can overlap in the upper parts of the lung with the pseudoglandular phase in lower parts. Respiration is possible at the end of the canalicular phase, after thin-walled terminal saccules have developed at the ends of the respiratory bronchioles. The whole lung is well vascularized at this stage, making gas exchange via diffusion possible. Preterm babies who develop BPD are usually born when the lung development is in the canalicular and/or early saccular phase. The later phases of lung development occur postnatally in the presence of injurious stimuli such as resuscitation, oxygen toxicity, sepsis and persistent ductus arteriosus. The preterm babies who were described by Northway and colleagues some 50 years ago were born in a later phase of lung development. Their lung development was already in the late saccular and early alveolar phase when the first alveoli developed. The terms ‘old’ and ‘new’ BPD, therefore, not only reflect the progress of perinatal medicine in the past decades, but also emphasize different stages of lung development in which preterm birth and subsequent extrauterine lung development occur.

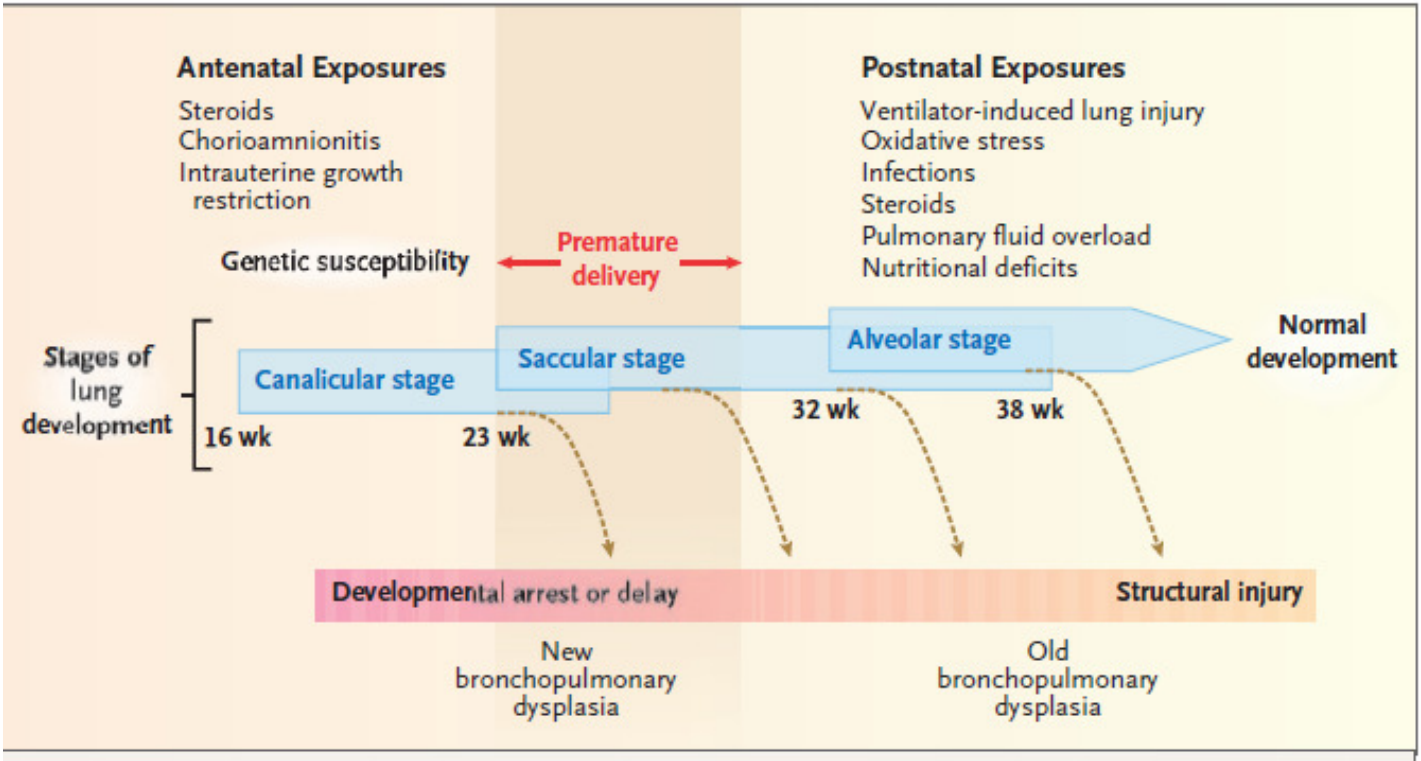

Figure 1. Stages of Lung Development, Potentially Damaging Factors, and Types of Lung Injury.

In premature newborns, the lungs are often exposed to several sources of injury, both before and after birth. Such exposures — as well as genetic susceptibility to problematic lung development — may cause direct airway and parenchymal damage and induce a deviation from the normal developmental path. Depending on the timing and extent of the exposures, lung injury may range from early developmental arrest (new bronchopulmonary dysplasia) to structural damage of a relatively immature lung (old bronchopulmonary dysplasia). Premature infants born at a gestational age of 23 to 30 weeks (region shaded light red) — during the canalicular and saccular stages of lung development — are at the greatest risk for bronchopulmonary dysplasia.

The newborn rat pup model is a very convenient model for studying various aspects of BPD (5).

At birth rats present with large primitive alveoli (saccular stage) with thick walls. At 4-5 days of life these strucutures are divided into smaller spaces by septae originating from the walls (alveolar stage). This process occurs during the first 2 weeks of life. The most rapid rate of alveolar formation occurs between days 3 and 8 of life and is largely completed by day 14. At the beginning of the 3rd week of life there is a remodelling of the alveoli with walls getting less thick than before. Similar postnatal modifications occur in human lung too.

Rats' lungs at birth are in saccular stage, whereas in humans, baboons and lambs alveolarization has already occurred at birth. As a matter of fact, the saccular stage of the newborn rat pup is compatible to the lung development of premature infants at 25 weeks of gestation. This is the reason why rat pups at term are a good model to study the process of alveolarization occuring during the last part of human pregnancy and which is incomplete when birth is premature.

Animal studies have shown that exposure to hyperoxia during the neonatal period causes lung structural changes that are similar to the histology seen in human infants with BPD (6, 7). Lung histology after hyperoxia is characterized by reduced complexity of the distal lung with decreased alveolar number and vascular growth (6,7).

Newborn rats exposed to 95% oxygen develop a homogeneous arrest of lung growth and DNA synthesis (8); newborn rats exposed to 60% oxygen for 14 days develop a heterogeneous parenchymal lung injury with areas of arrested alveolarization and growth mixed with patchy areas of interstitial thickening with active DNA synthesis (9). and small airspaces interspersed with areas of enlarged airspaces (10).

The lungs of newborn rats exposed to 60% oxygen for 14 days develop an injury that shares morphologic similarities to human bronchopulmonary dysplasia (BPD).

Recent studies in premature baboons (11) leave little doubt that oxidant injury alone can produce the pathologic features of BPD. It is not clear whether the major oxidant stress is derived from excess reactive oxygen species formed in constitutive lung cells under hyperoxic conditions, or from phagocytes invading the lung as part of the inflammatory process induced by hyperoxia (12).

Hyperoxia also reduces endothelial nitric oxide (NO) synthase expression in the lung, and the production of NO, which is a crucial downstream effector of the angiogenic vascular endothelial growth factor (VEGF) (13, 14).

NITRIC OXIDE AND LUNG DEVELOPMENT

Growth of the pulmonary circulation and alveolarization are closely coordinated events occuring during lung morphogenesis (15) and NO has been proven to be a critical regulator of lung morphogenesis and homeostasis during fetal life (16).

Nitric oxide improves gas exchange, decreases lung inflammation and oxidant stress and enhances angiogenesis and growth in the immature lung.

The potential role of inhaled NO in the prevention of BPD has been recently studied, but not yet clearly defined. Inhaled NO therapy improves lung pathology, reduces fibrin deposition and pulmonary inflammation, and prolongs survival in an animal model of BPD (17). NO plays an important role in regulating pulmonary vascular tone and alveolar capillary development and in reducing inflammation in the developing lung (18,19); NO enhances distal lung growth after exposure to hyperoxia in neonatal rats (18). In addition to the acute effects of iNO on pulmonary vasodilation, lung inflammation, and oxidant stress, there is increasing evidence that impaired endogenous NO production contributes to the pathogenesis of BPD. For example, lung endothelial nitric oxide synthase (eNOS)

expression is decreased in ovine and primate models of BPD (20). The potential for iNO to modulate the evolution of lung injury in animal models of BPD has been the focus of recent studies, providing further experimental rationale for the role of iNO in premature subjects. Lin et al found that hyperoxia inhibited lung vascular growth and impaired alveolarization in neonatal rats, and that treatment with iNO after neonatal hyperoxia enhanced late lung growth and improved alveolarization in this model of BPD(18). Mc-Curnin et al studied the effects of iNO in a baboon model of BPD over the first 14 days of life (19). They found that iNO partially improved early pulmonary function, lung structure, and extracellular matrix deposition in mechanically ventilated premature baboons with evolving BPD. In chronically ventilated premature lambs, Bland et al found that iNO administration preserved structure and function of airway smooth muscle and enhanced alveolar development (21). Thus, compelling evidence suggests that endogenous NO plays a vital role in pulmonary vascular and alveolar development in the immature lung, and that low-dose iNO may have beneficial effects on both the acute and chronic perturbations that are associated with the pathogenesis of BPD in the premature newborn.

However, the pathways mediating NO prevention of lung growth alteration have not been fully elucidated. A likely potential therapeutic target for NO prevention of BPD is angiogenesis. Lung alveolar development is intimately related to vascular growth, and NO has been shown to enhance angiogenesis in ischemic tissues (22). In ischemic brain, this effect was demonstrated to be partly mediated via the synthesis of VEGF (23). Moreover, recombinant VEGF treatment has recently been shown to enhance alveolarization after hyperoxia (24).

NITRIC OXIDE, L-ARGINE AND L-CITRULLINE

Nitric oxide synthase converts L-arginine to NO and L-citrulline (25).

Oral supplementation with L-arginine has been shown to enhance NO-mediated vasodilation in several clinical studies (26,27) but not in all (28).

After oral administration, L-arginine is subject to extensive presystemic and systemic elimination, i.e. by bacteria in the gut and arginases in the gut and liver, respectively (29).

The non-essential amino acid L-citrulline is not subject to presystemic elimination but to systemic metabolism. L-Citrulline is converted to L-argininosuccinate by argininosuccinate synthase and subsequently to L-arginine by argininosuccinate lyase (30). It may therefore serve as an L-arginine precursor (31) and many NO producing cells (vascular endothelial cells and macrophages) use L-citrulline as substrate to form L-arginine.

Citrulline takes its name from the Latin for watermelon, Citrullus vulgaris, which contains large amounts of this amino acid.

Citrulline has long been administered in the treatment of inherited urea cycle disorders, and recent studies suggest that citrulline may be used to control the production of NO.

Citrulline metabolism in mammals is divided into two fields: free citrulline and citrullinated proteins. Free citrulline metabolism involves three key enzymes: NO synthase (NOS) and ornithine carbamoyltransferase (OCT) which produce citrulline, and argininosuccinate synthetase (ASS) that converts it into argininosuccinate. The tissue distribution of these enzymes distinguishes three ‘‘orthogonal’’ metabolic pathways for citrulline. Firstly, in the liver, citrulline is locally synthesized by OCT and metabolized by ASS for urea production. Secondly, in most of the tissues producing NO, citrulline is recycled into arginine via ASS to increase arginine availability for NO production. Thirdly, citrulline is synthesized in the gut from glutamine (with OCT), released into the blood and converted back into arginine in the kidneys (by ASS); in this pathway, circulating citrulline is in fact a masked form of arginine to avoid liver captation. Each of these pathways has related pathologies and, even more interestingly, citrulline could potentially be used to monitor or treat some of these pathologies.

Citrullinaemia seems to vary with age, but not with alimentation (32).

Two enzymes are mainly responsible for citrulline synthesis, corresponding to the two main metabolic pathways in which it is involved: ornithine carbamoyltransferase and NO-synthase (including all its iso-enzymes). Only one enzyme, argininosuccinate synthase is capable of citrulline catabolism in mammals, and it is used in both metabolic pathways. Citrulline contained in food is absorbed by the intestine. Most of the circulating citrulline comes from glutamine conversion in enterocytes (33). If it is not used in NO metabolism, citrulline is mainly metabolized in the kidney, where it is converted into arginine by cells of the nephron proximal tubules (34). Conversion in the kidney is achieved through a partial urea cycle involving ASS and argininosuccinate lyase (ASL). Synthesized arginine is released into the general blood circulation.

In adults, the citrulline converted by the kidney is enough to provide the body's full arginine requirements. Arginine synthesized from citrulline represents 60% of the de novo arginine synthesis in the organism, but only 5 to 15% of circulating arginine (35). The main reason for this citrulline metabolism split between two organs is related to the efficacy of the capture of arginine by the liver. In fact, without metabolic adaptation, almost all the arginine coming from food supply would be withdrawn from the portal blood by the liver, leaving only very low amounts of available arginine for other organs. Citrulline is the solution to this problem: it can be seen as a masked form of arginine to bypass the liver. Because citrulline is easily converted into arginine by a half urea cycle with the action of ASS and ASL, it can be used as a precursor of NO. Hence, many cell types which are able to metabolize arginine into NO are able to uptake circulating citrulline, which explains why citrulline induces certain of the NO effects; for example, it can decrease the tonicity of blood vessel muscles (36).

This citrulline can also be supplied by arginine conversion into NO itself, forming the so-called NO cycle. In activated macrophages, this citrulline recycling accounts for up to 20%

of NO produced (37). The ability of citrulline to restore blood arginine levels was first reported by Hartman et al. (1994), and this idea is now explored in several ways (38).

Oral L-citrulline may lead to higher elevations of plasma L-arginine concentrations than administration of L-arginine itself.

More and more studies have shown that citrulline can act as an arginine precursor: in a recent double-blind, randomized, placebo-controlled cross-over study, L-citrulline was demonstrated to increase, in a dose-dependent way, AUC and Cmax of plasma L-arginine concentration more effectively than L-arginine ($P < 0.01$)(39).

There is evidence suggesting that L-citrulline administration may attenuate arrested alveolar growth and pulmonary hypertension in extreme hyperoxia lung injury in newborn rats (40).

We hypothesized that administration of L-citrulline, raising plasma and tissue levels of L-arginine and enhancing endogenous NO production, might attenuate hyperoxia-induced lung injury in an experimental model of BPD obtained by exposure to moderate hyperoxia.

VEGF

VEGF has a pivotal role in the proper homeostasis of the endothelial and alveolar barrier. It has been demonstrated that VEGF blockade after birth reduces vascular and alveolar growth in rats (15) and leads to an emphysema phenotype in mice (41). VEGF is required not only for the formation, but also for the life-long maintenance of the pulmonary vascular architecture and alveolar structure (14).

Neonatal hyperoxia reduces lung VEGF mRNA and protein expression, suggesting that downregulation of VEGF may contribute to the simplified lung structure seen in this model (42,43).

Recent studies further suggest that the reduction in VEGF protein persists beyond the hyperoxic injury and into the recovery period (18).

It has been shown that late treatment with VEGF after hyperoxia can improve lung growth during recovery (44). VEGF may have a direct effect on angiogenesis and alveolarization through liberation of nitric oxide (NO) (45, 46).

In addition, studies have shown a persistent reduction in VEGF protein following neonatal hyperoxic lung injury despite recovery in room air and that inhaled nitric oxide (iNO) preserves normal lung growth after disruption of VEGF signaling (47).

Several studies have also shown that lung endothelial nitric oxide synthase is also reduced in animal models of BPD (48, 49). Previous studies have demonstrated that iNO during hyperoxia exposure may reduce acute lung injury in several animal models (50, 51, 52).

These studies collectively suggest a critical role for the VEGF-NO signalling pathway during normal early postnatal lung development. Alternatively, VEGF may have a direct effect on the pulmonary epithelium in promoting alveolarization. Studies have shown that VEGF may be involved in epithelial growth in fetal human lung explants in vitro and that exogenous VEGF can increase epithelial proliferation (53).

MMPs

The lung development and repair processes also involve the matrix metalloproteinases (MMPs). Among the MMPs produced, MMP2 is known to play a key part in lung development and repair after injury. MMP2 is also involved in initiating angiogenesis and could promote the release of extracellular matrix-bound cytokines, such as VEGF (54).

MMPs are a group of proteases that exist as pro-enzymes and are cleaved by other MMPs to active forms that have several specialized functions, including extracellular matrix turnover. Some of their functions regulate processes associated with development, such as branching morphogenesis and angiogenesis as well as inflammatory processes and wound healing (55).

MMP-2 and MMP-9, also called gelatinases-A and -B, respectively, cleave gelatin, type IV and V collagen, and elastin. Types IV, V, and VII collagens are associated with basement membranes (56).

Among secreted MMPs, MMP2 is known to play a key role in lung development and repair after injury. Mice lacking MMP2 show delayed alveolar development (57), and low MMP2 levels in tracheal effluent and plasma have been linked to an increased risk of BPD in infants (58,59).

MMP-2 and MMP-9 exhibit increased gelatinolytic activities as the lung develops (60), and during the postnatal lung growth stage both MMP-2 and MMP-9 are detected in alveolar epithelial cells. MMP-2–deficient mice develop normally, with no gross anatomical abnormali ties, however, they display a significantly slower growth rate (approximately 15%) (61).

MMPs are tightly regulated by the TIMP. Four different TIMP have been characterized: MMP-9 pro-enzyme and active enzyme bind TIMP-1 most avidly and TIMP-2 and -3 less so. TIMP-2, -3, and -4 bind with high affinity to MMP-2. TIMP-1 is inducible whereas TIMP-2 is constitutive. It is likely that TIMP play key roles in maintaining the balance between extracellular matrix deposition and degradation (62).

Because MMPs degrade growth factors, these effects of TIMP-1 may result from its inhibition of MMPs and prevention of growth factor degradation.

Hyperoxia has been shown to alter pulmonary MMPs. Adult rats exposed to 85% O_2 had increased levels of MMP-2 and MMP-9 activities in both bronchoalveolar lavage fluid and type II cells (63).

Materials and Methods

Animals

The study was conducted on male and female Sprague-Dawley (SD) (Harlan, Udine, Italy) rat pups in conventional facilities in accordance with the recommendations of the Italian Public Health Service, law 116/92. Mothers and litters were placed in clear polished acrylic chambers (BioSpherix, OxyCycler model A84XOV, Redfield, NY) where the oxygen concentration was set for 14 days at 60% FiO_2, with a software enabling a continuous monitoring of O_2 and CO_2. Animals were fed ad libitum and exposed to alternating 12 h day-night cycles.

Experimental design

A total number of 50 newborn rats were randomly distributed between four experimental groups:

Group 1 (room air, n=10), raised in room air for 14 postnatal days and used as a control group;

Group 2 (hyperoxia, n=12), exposed to 60% O_2 for 14 postnatal days;

Group 3 (L-citrulline+hyperoxia, L-citr+hyperoxia, n=18), exposed to 60% O_2 and treated with intraperitoneal L-citrulline daily for the first 14 days of life;

Group 4 (hyperoxia+vehicle, sham, n=10), exposed to 60% O_2 and intraperitoneally administered a vehicle daily for the first 14 days of life.

L-citrulline ≥ 99.9% (NT) (Sigma, St. Louis, MO, USA) solution dissolved in NaCl 0.9% w/v at a final concentration of 0.1 mg/µl was administered once a day at a dose of 1 g/kg. The vehicle consisted of NaCl 0.9% w/v administered in the same volume as the drug. The study design is shown in Figure 1.

Tissue and fluid collection

On the 14th post-natal day, the animals were deeply anesthetized and killed with a 1:1 combination of zoletil and xylazine. Blood samples were centrifuged at 8000 rpm for 20 minutes at 4°C and serum was then separated and stored at –80°C. Bronchoalveolar fluid (BALF) was collected from the animals in each group after instilling 0.5 ml of 0.9% NaCl solution into the trachea through a 0.5 F catheter (Vygon Corporation); the fluid was centrifuged at 1500 rpm for 10 minutes and then stored at –80°C. The animals' tracheas were then cannulated and 4% neutral buffered formalin was instilled at a pressure of 25 cmH2O during a 5 min period of equilibration. The right lungs were then removed and fixed overnight in buffered formalin, washed in phosphate buffered saline, serially dehydrated in increasing concentrations of ethanol and embedded in paraffin. Left lungs were excised, freeze-clamped in liquid nitrogen and stored at -80°C for molecular studies.

Lung histology and morphometric analysis

Lung sections 4 µm thick were stained with hematoxylin and eosin. For each case studied, we examined five sections and three fields per section. Photomicrographs were obtained on a field of 568 µm X 422 µm at 20X magnification with a Leica DM 4000B microscope (Leica, Solms, Germany) integrated with a camera (Leica DFC 280). Lung morphometric analyses were performed by two independent researchers blinded to the treatment strategy, using ImageJ, a public domain Java image-processing program created by Wayne Rasband at the Research Services Branch, National Institute of Mental Health, Bethesda, MD (http://rsb.info.nih.gov/ij). In particular, alveolarization was determined by evaluating the number of alveoli/mm^2 according to Scattoni et al. (64).

Immunohistochemistry

Immunohistochemical staining was done using a Bond Max automated immunostainer (Leica Microsystems, Newcastle upon Tyne, UK). Tissue sections were dewaxed and rehydrated by successive incubation at 72°C in Bond Dewax Solution (Leica), ethanol, and distilled water. Antigens were retrieved by heating sections for 20 minutes at 100°C in Bond Epitope Retrieval Solution 2 (Leica). Endogenous peroxidase was blocked by adding 3% hydrogen peroxide prior to 15 minutes of incubation with rabbit polyclonal anti-vascular endothelial growth factor (VEGF) (catalog number sc-152 - VEGF-A20, 1:500; Santa Cruz Biotechnology, Inc., Santa Cruz, CA, USA). Specimens were then washed with phosphate-buffered saline (PBS) and incubated with Bond Intense R Detection Kit (Leica) according to the manufacturer's instructions. The staining was visualized with 3,3'-diaminobenzidine (DAB) and the slides were counterstained with hematoxylin. The sections were then dehydrated, cleared, and mounted. Formalin-fixed, paraffin-embedded normal lung was used as a positive control. Negative controls were obtained using an identical staining procedure while substituting primary buffer for primary antibody.

RT and real-time quantitative PCR Total RNA was isolated using TRIzol reagent according to the manufacturer's instructions (Invitrogen, Carlsbad, CA, USA). Samples were further treated with DNase 1 (DNA-free, Ambion, Austin, TX, USA) to ensure there was no DNA contamination. RNA quality was assessed by formaldehyde agarose gel electrophoresis.

Reverse transcription

Total RNA (100 ng) was added to a reaction mixture containing 100 ng random nanomers (Stratagene, La Jolla, CA, USA.), 1X cDNA first-strand buffer, 500 mM DTT, 0.4 U/μL RNase inhibitor, 1 mM each of deoxyribonucleoside triphosphate (dNTP) and 0.75 U/μL Superscript II reverse transcriptase (Invitrogen). Negative RT (with no enzyme) and no-

template controls were also included. The RT thermal cycle was 25°C for 10 min, 50°C for 45 min, and 85°C for 5 min.

Quantitative real-time PCR

We performed a quantitative real-time PCR assay based on the use of SYBR Green I (Applied Biosystems) as the fluorescent intercalation dye in double-stranded DNA during the amplification cycles. The assays were performed in 96 multi-well PCR plates covered with optical tapes in the Applied Biosystems 7500 Real-Time PCR System in a final volume of 25 µl, containing 10 ng of cDNA, 12.5µl of Power Master Mix 2X (Applied Biosystems), 5 µmol of either VEGF, MMP2 or GAPDH forward and reverse primers, and water. The specific primer sequences are listed in Figure 1/B. The reaction underwent denaturation at 95°C for 10 minutes followed by 40 cycles of denaturation at 95°C for 30 seconds, annealing and elongation at 60°C for 1 minute. mRNA expression levels were evaluated using a relative quantitative real-time PCR in each lung of the experimental group and normalized to GAPDH. The comparative Ct method ΔΔCt) was used to quantify gene expression and the relative quantification (RQ) was calculated as 2-ΔCt (22). The gene expression level in the animals raised in room air was considered as 100%; VEGF and MMP2 levels in the other samples were calculated relative to said value.

Zymographic analysis of MMP2 gelatinase activity

Zymographic analysis was performed on BALFs using a standard procedure. Equal amounts of BALF in sample buffer (4% SDS, 125 mM Tris-HCl pH 6.8, 20% glycerol and 0.05% bromophenol blue) were resolved under non-reducing conditions on 10% SDS-PAGE gels copolymerized with 0.1% gelatin. After electrophoresis, the gels were washed for 30 minutes in 2.5% Triton X-100 at room temperature to remove SDS, then equilibrated in collagenase buffer (50 mM Tris, 200 mM NaCl, 5 mM CaCl2 and 0.02% Triton X-100,

pH 7.4) for 30 minutes and finally incubated overnight with fresh collagenase buffer at 37℃. After incubation, gels were stained in 0.1% Coomassie Brilliant Blue R-250 30% MetOH/10% acetic acid for 1 hour and destained in 30% MetOH/10% acetic acid. Clear bands on the blue background represented areas of gelatinolysis. Digestion bands were analyzed by ImageJ (65).

Assessment of serum arginine

Serum arginine concentrations were determined using an HPLC method with pre-column derivatization and fluorescence detection. Sample preparation consisted of SPE (solid phase extraction) and derivatization. Before analysis, 200 µL of thawed sample (calibrator, control or animal sample) were diluted with 600 µL of PBS (10 mM sodium phosphate, 140 mM NaCl, pH 7.0), after which 200 µL of the internal standard (monomethyl arginine, 10 µmol/L) was added and mixed by vortexing for 30 s. The cartridges were first conditioned with 1 mL elution buffer (10/0.5/40/50; NH3 concentrated/1 M NaOH/bidistilled water/CH3OH; v/v/v/v) followed by 1 mL bidistilled water, before they were loaded with the diluted sample. Washing with 1 mL 0.1 M HCl was followed by 1 mL CH3OH. Arginine and its metabolites were eluted with 1 mL of elution buffer. All conditioning, washing and elution steps where achieved by vacuum suction. The collecting speed was 2 mL/min; all other steps were completed at a rate of 15 mL/min. The eluate was blow-dried with nitrogen gas (45 ℃). The residue was dissolved with 100 µL of derivatization reagent (prepared by dissolving 10 mg of OPA in 0.2 mL CH3OH, followed by the addition of 3.8 mL of a 0.2 M potassium borate buffer (pH 9.5) and 10 µl of 3-mercaptopropionic acid); 100 µL of 0.2 M KH2PO4 was added after completing the derivatization reaction (which took at least 60 s). After mixing for 30 s, the samples were transferred to autosampler vials and placed in the refrigerated samples compartment of the separation module. The HPLC equipment consisted of an Agilent 1100 (Agilent Technologies, California, USA) and a

model RF-10AXL fluorescence detector from Shimadzu (Japan). Chromatographic separation (30 µL injection volume) was achieved at 35℃ on a Chromolith Performance RP-18 (100×4.6 mm) with a guard cartridge (10×4.6 mm) supplied by Merck (Darmstadt, Germany). The mobile phase A consisted of 25 mM of phosphate buffer (pH 6.5) containing 7% CH3CN, and the mobile phase B of CH3CN/bidistilled water (50:50). Separation was performed isocratically for 100% of the mobile phase A, at a flow rate of 1.5 mL/min. After elution of the SDMA, the mobile phase was switched to 100% mobile phase B, and the flow rate was raised to 2.0 mL/min to elute strongly retained compounds. Fluorescence was monitored at an excitation rate of 340 nm and an emission rate of 455 nm.

Statistics

Results are presented as mean±SEM. Differences were analyzed by two-way ANOVA, and a p value <0.05 was considered statistically significant. Calculations were done using Statgraphics (Software Inc., Padova University, Italy).

Results

No pups died during oxygen exposure and all gained weight throughout the first 14 days after birth. Body weights did not differ between room air, hyperoxic, sham and L-citrulline treated animals.

Serum arginine levels

The mean serum arginine level (µmol/L) was higher in the L-citr+hyperoxia group than in the other groups: room air = 262.56 ± 9.19 µmol/L; hyperoxia 275.3 ± 10.79 µmol/L; L-citr+hyperoxia treated group = 303 ± 32.71 µmol/L; sham = 276.04 ± 9.81 µmol/L, $p<0.05$ (Figure 2).

Morphometric analysis

Exposure to 60% hyperoxia during the first 14 days after birth was associated with an arrested alveolarization, inducing a change in lung morphology with patchy areas of parenchymal thickening interspersed with areas of enlarged air spaces. The lung sections of the L-citr+hyperoxia rats contained smaller and more numerous air space units, and were more similar to the lungs of the room air group. There was no evidence of inflammatory cells, but the septa were thicker in the hyperoxic and sham groups than in the room air and L-citr+hyperoxia groups (Figure 3/A). The number of alveoli per mm^2 14 days after birth was significantly higher in the L-citr+hyperoxia group (40.15 ± 4.10) than in the hyperoxia group (29.17 ± 2.89) or the sham group (32.27 ± 2.11, $p<0.05$), while it was not different from that of the room air group (38.51 ± 2.85) (Figure 3/B).

MMP2 mRNA levels and active MMP2 zymography

MMP2 gene expression 2 weeks after birth did not differ significantly between the groups (Figure 4/A): room air = 100 ± 11.97%/GAPDH; hyperoxia = 98.85 ± 6.53%/GAPDH; L-citr+hyperoxia treated group= 111.07 ± 7.64%/GAPDH; sham = 78.82 ± 20%/GAPDH, $p>0.05$. Using gelatinase zymography on BALFs, there was a clearly evident, marked band corresponding to active MMP2 in all groups: room air = 100 ± 15.10% arbitrary units; hyperoxia = 66.04 ± 5.41% arbitrary units; L-citr+hyperoxia treated group = 102.72 ± 13.78% arbitrary units; sham = 52.70 ± 8.15% arbitrary units. In particular, MMP2 activity levels differed significantly between the L-citr+hyperoxia group and the hyperoxia group (being approximately 40% higher in the former) and sham groups (approximately 50% higher), $p <0.05$ (Figure 4/B).

VEGF expression

VEGF expression (%) in the hyperoxia and sham groups was lower than in the L-citr+hyperoxia or room air groups, $p<0.05$ (Figure 5): room air = 100 ± 15.74%/GAPDH; hyperoxia = 54.81 ± 3.28%/GAPDH; L-citr+hyperoxia = 75.71 ± 5.28%/GAPDH; sham = 44.47 ± 13.10%/GAPDH. The hyperoxia and sham groups had a weaker VEGF immunostaining than the L-citr+hyperoxia and room air groups. This pattern validates the VEGF real-time expression profile (Figure 6).

Discussion

The purpose of this study was to explore the effects of L-citrulline treatment on lung development in rat pups exposed to hyperoxia during the first 2 weeks of life.

In rats, alveolarization is mainly completed in 14 days after birth, a period corresponding in our model to a lung development midway between alveolar and microvascular maturation. The lungs of newborn rats exposed to 60% oxygen for 14 days develop an injury that bears a morphological resemblance to human BPD (10,66).

Our hypothesis was that administering L-citrulline may enhance NO production and reduce hyperoxia-induced damage to the developing lung.

Compelling evidence suggests that endogenous NO plays a vital role in pulmonary vascular and alveolar development in the immature lung. As a matter of fact, NO has various biological effects; in particular it enhances angiogenesis and growth in the immature lung. NO is produced by endothelial NO synthase (eNOS) in the pulmonary vascular endothelium using L-arginine as a substrate and producing L-citrulline as a by-product. In turn, L-arginine can be synthesized from L-citrulline, providing a recycling pathway for the conversion of L-citrulline to NO via L-arginine (67).

It has been shown that providing L-arginine to endothelial cells increases NO production only slightly compared with the more dramatic increase in endothelial NO production found with L-citrulline supplementation (67).

It has recently been shown that L-citrulline supplementation reduces pulmonary hypertension and increases NO production in piglets exposed to chronic hypoxia (68), and may attenuate both pulmonary hypertension and alveolar growth derangement in hyperoxia-induced lung injury in newborn rats (40).

It is well known that L-citrulline is converted into arginine and serves as its precursor. We consequently measured serum arginine concentrations first. As expected, arginine levels

were found increased in the treated group, demonstrating the efficacy of the dose we used. All animals gained weight normally and were breast fed with no evident side effects in the group administered with L-citrulline.

In our study, rats exposed to hyperoxia during the first 14 days of life developed lung lesions, such as patchy areas of parenchymal thickening interspersed with areas with enlarged air spaces. L-citrulline treatment seemed to prevent the changes in lung morphology induced by moderate hyperoxia. In particular, our treatment was associated with an increased alveolarization, as demonstrated by the higher number of alveoli/mm^2.

This preliminary finding prompted us to study specific markers of lung development to better characterize the effects of L-citrulline.

In particular, VEGF plays a crucial part in the proper metabolism of the endothelial and alveolar barrier; it is a potent proangiogenic and endothelial survival factor (13, 69).

A finding worth emphasizing in our results was that VEGF expression in the L-citrulline treated lung was similar to the room air control group, while it was lower in the untreated groups exposed to hyperoxia. This result was confirmed by the higher prevalence of VEGF-positive cells found in the lungs of the treated animals than in those not treated.

It has been reported that NO is a powerful downstream VEGF controller (70), but the exact relationship between NO and VEGF is still not clear, since it appears that NO might also take effect upstream from the VEGF (71). Further studies are needed to understand the factors regulating NO/VEGF signaling and L-citrulline administration.

Alveolarization is known to require coordination between several factors, particularly an optimal interaction between extracellular matrix remodeling and epithelial morphogenesis and capillary growth (72). It has also been recognized that the lung matrix plays an active role in inflammatory response, and consequent remodeling in several lung diseases involves MMPs (73, 74). Our study showed that MMP2 gene expression 14 days after birth was much the same among the study groups, but MMP2 protein activity (as measured by

BALF zymography) was higher in the L-citrulline treated group than in the hyperoxia or sham groups. Since MMP2 has a complex, tightly regulated secretion and activation system, our results seem to suggest that L-citrulline does not influence gene expression, but may regulate BALF MMP2 at post-transductional level. It has been reported that mice lacking this proteinase have a delayed alveolar development (57) and low MMP2 levels in BALF and plasma have been linked to an increased risk of BPD in infants (58, 59), so a higher level of MMP2 in BALF after L-citrulline administration might have a protective effect against hyperoxia-induced lung derangement.

In conclusion, our main findings were that: (i) administering L-citrulline proved effective in improving alveolar growth in a situation of oxygen-induced lung damage; (ii) such a result might conceivably relate to the arginine conversion pathway of L-citrulline. The mean serum arginine concentration was higher in our L-citrulline treated group, in which a greater alveolar growth was also noted; (iii) VEGF gene expression also increased in our L-citrulline treated group, coupled with a higher MMP2 enzyme activity in the BALF.

Bearing in mind that the main effect of L-citrulline is an increase in arginine levels, as a promoter and a substrate of nitric oxide synthase, a protective effect on alveolar and matrix maturation is feasible in our model and would seem to be promising with a view to BPD prevention strategies.

FIGURES

A

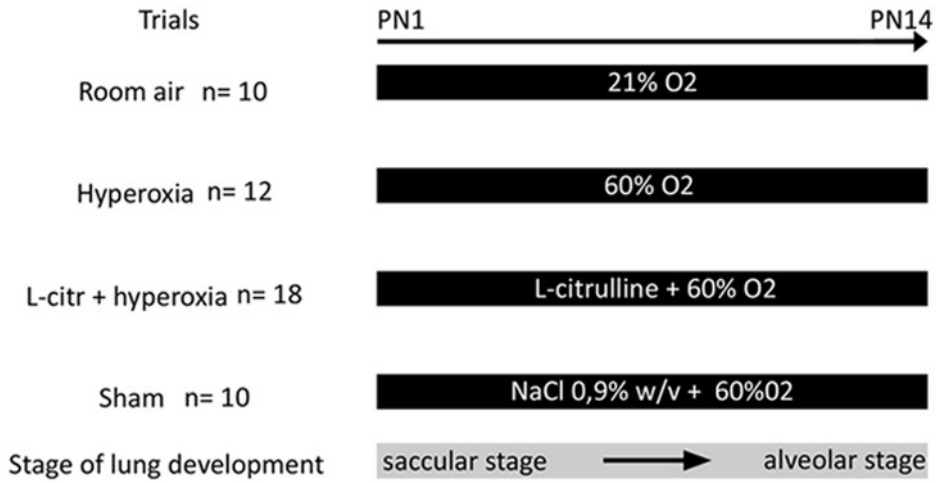

B

Gene	sequences
VEGF	d - ATGACGAGGGCCTGGAGTGTG r - CCTATGTGCTGGCCTTGGTGAG
MMP2	d-TGCCATCCCTGATAACCTGGAT r - CTCCTTCAGACTTTGGTTCTCC
GAPDH	d-TGAGGACCAGGTTGTCTC r--ACAGCGTCGAATCCTTTGAG

Fig. 1/A: Schematic outline of the experimental design. PN = postnatal day; black bars indicate the study groups, i.e. room air, n = 10; hyperoxia, n= 12; L-citr+hyperoxia, n = 18; sham, n = 10. The stage of lung development corresponds to the saccular phase on PN1, becomes mainly alveolar by PN14 (grey bar).

Fig. 1/B: Nucleotide sequences of the primers used for real-time PCR analyses.

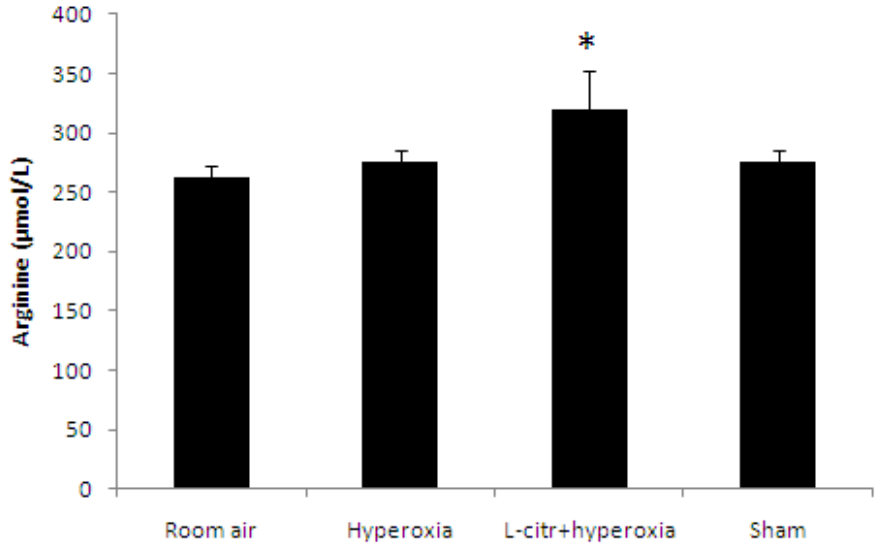

Fig: 2: Mean serum arginine (µmol/L) was higher in the L-citr+hyperoxia group at PN14 than in the other study groups. Data are mean ± SEM. * indicates that arginine rose in the L-citr+hyperoxia group, $p < 0.05$.

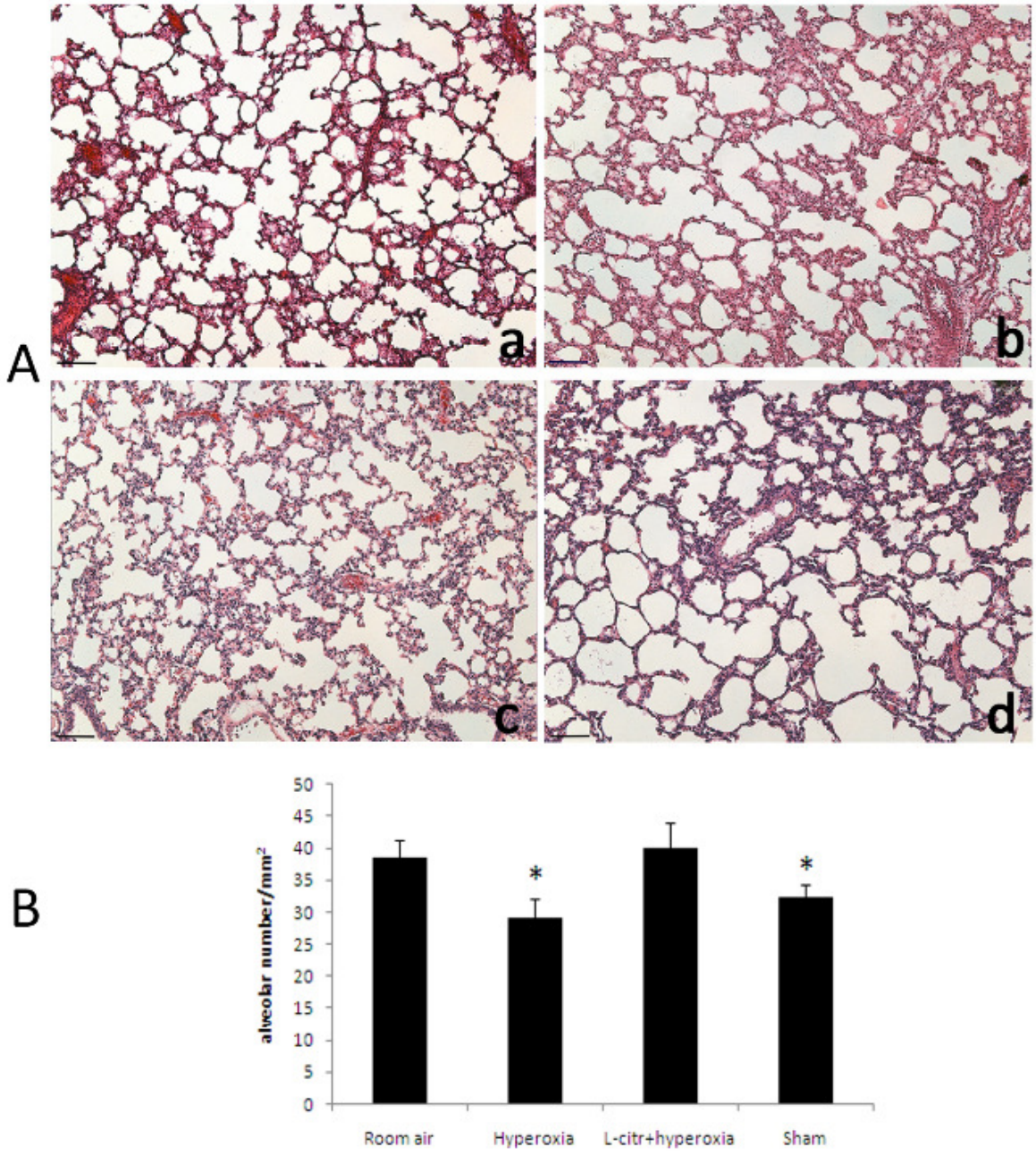

Fig. 3/A Photomicrographs of rat lung parenchyma 2 weeks after birth. Exposure to 60% hyperoxia (b) and sham (d) groups were associated with arrested alveolarization, inducing heterogeneous changes in lung morphology with patchy areas of parenchymal thickening and enlarged air spaces. Lung sections of L-citr+hyperoxia (c) rats contained smaller, more numerous alveoli and were comparable with those of the room air group (a). Scale bars = 100 µm.

Fig. 3/B Morphometric analysis (number of alveoli per mm^2) of rat study groups at PN14. Data are mean ± SEM. * indicates that the number of alveoli per mm^2 was lower in the hyperoxia and sham groups than in the room air and L-citr+hyperoxia groups, $p<0.05$.

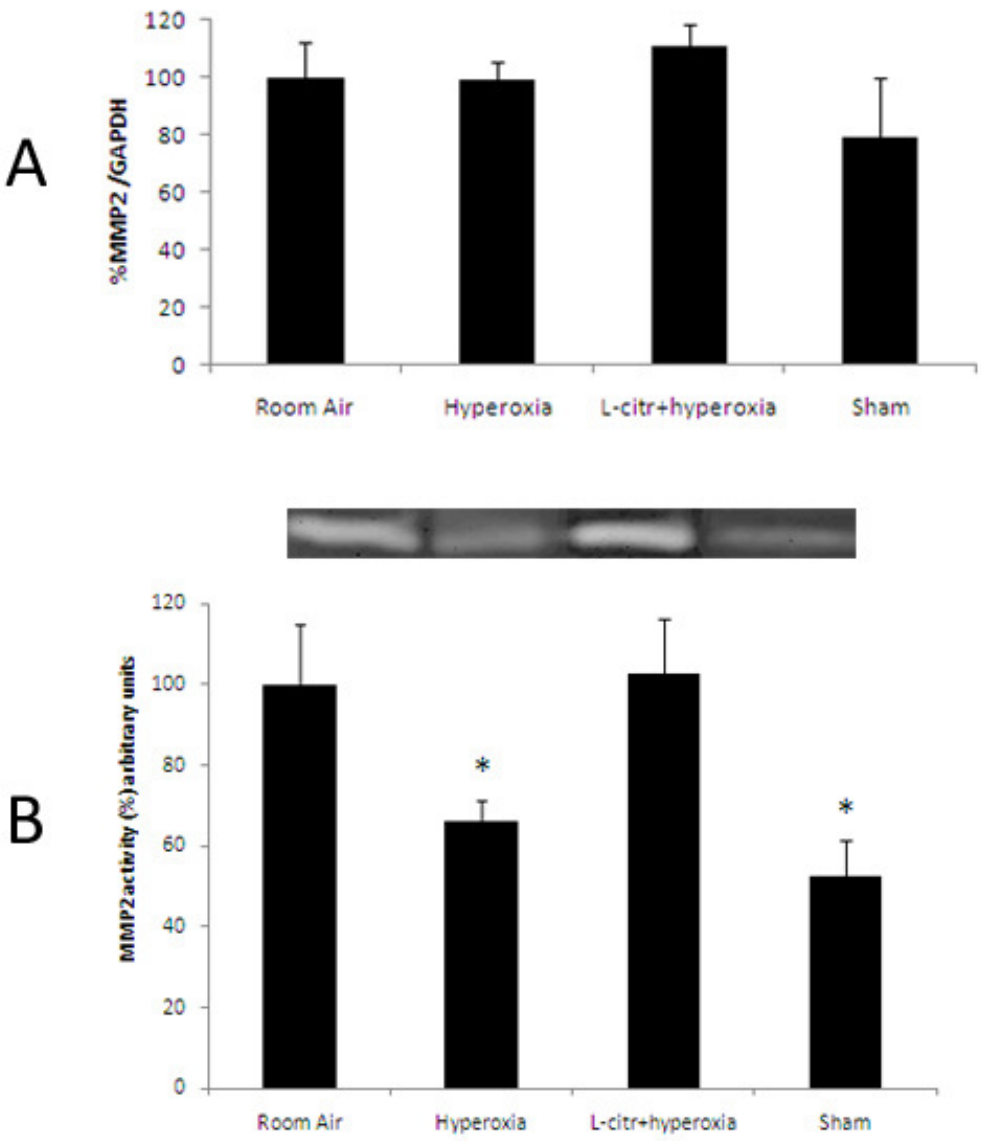

Fig 4/A: Real-time PCR analysis showed that the rats' lung expression of MMP2 at PN14 did not differ significantly between the study groups. Data are mean ± SEM and normalized to 100% (room air group).

Fig 4/B: Active MMP2 BALF levels at PN14 measured by gelatinase zymography bands. Histograms show the quantification of clear areas of gelatinolysis. * indicates that active MMP2 BALF levels were lower in the hyperoxia and sham groups than in the room air and L-citr+hyperoxia groups, $p<0.05$. Data are mean ± SEM and are normalized to 100% (room air group).

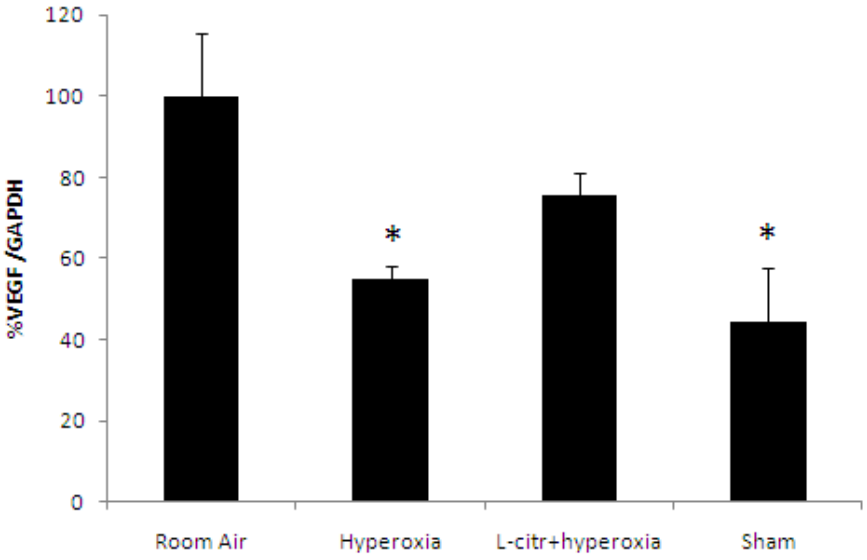

Fig 5: Real-time PCR analysis of lung VEGF expression in the study groups at PN14. * indicates that VEGF expression was lower in the hyperoxia and sham groups than in the room air and L-citr+hyperoxia groups, $p<0.05$ Data are expressed as mean ± SEM and are normalized to 100% (room air group).

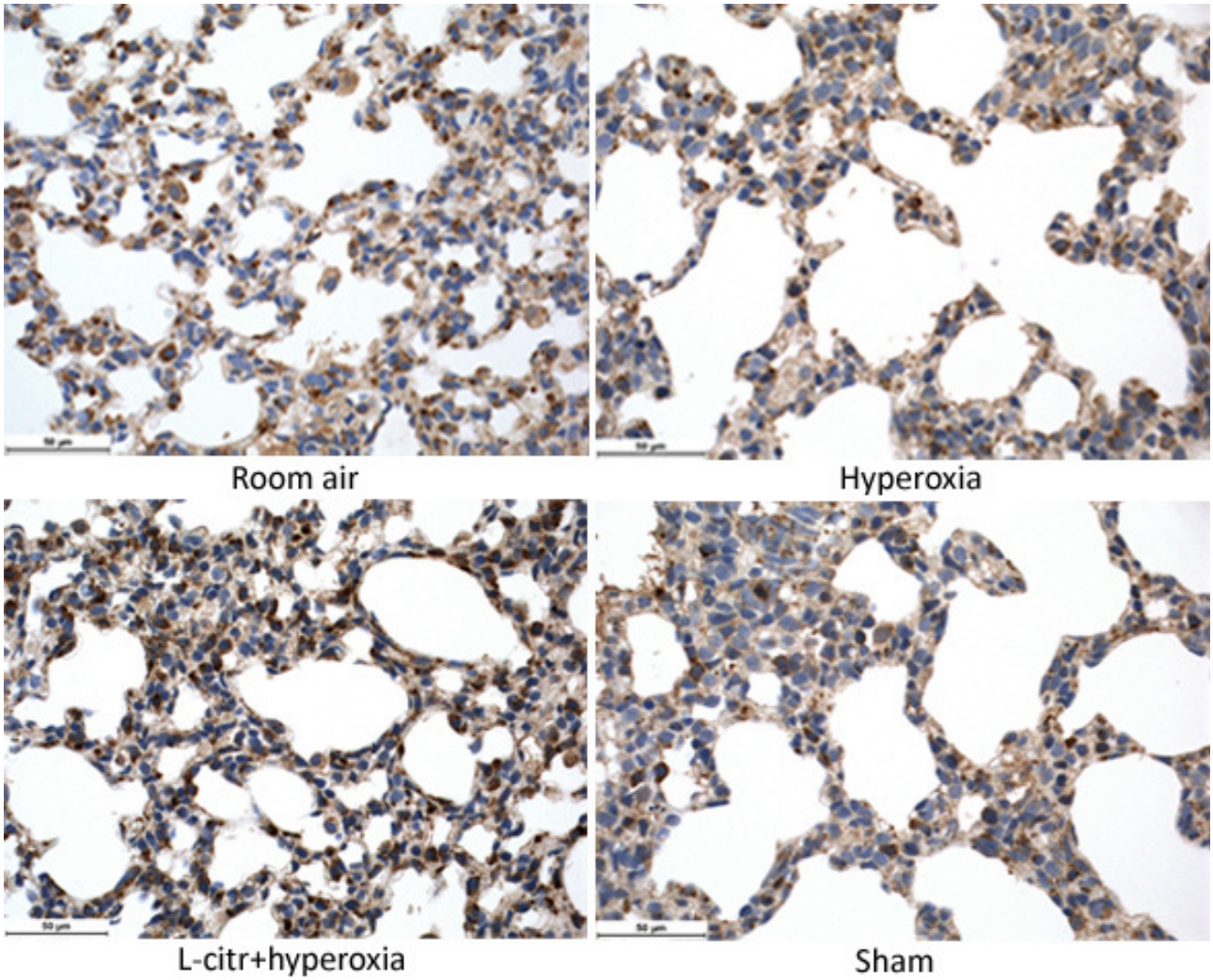

Fig. 6 Photomicrographs of rat lung parenchyma at PN14. VEGF immunochemistry (brown-stained cytoplasm) was observed mainly in alveolar and endothelial cells. The hyperoxia and sham groups had weaker VEGF immunostaining than the L-citr+hyperoxia and room air groups. This pattern is consistent with the VEGF real-time expression profile. Scale bars = 50 µm.

REFERENCES

1. **Northway WH**, Rosan RC, Porter DY. Pulmonary disease following respiratory therapy of hyaline membrane disease: bronchopulmonary dysplasia. N Engl J Med 1967;276:357–68.

2. **Jobe AH, Bancalari E**. Bronchopulmonary dysplasia. Am J Respir Crit Care Med 2001;163:1723–9.

3. **Jobe AH.** The new BPD: an arrest of lung development. Pediatr Res 1999; 46: 641–643.

4. **Burri PH.** Structural aspects of postnatal lung developmentFalveolar formation and growth. Biol Neonate 2006; 89: 313–322.

5. **Tanswell AK**, Wong L, Possmayer F, Freeman BA. The preterm rat: a model for studies of acute and chronic neonatal lung disease. Pediatr Res. 1989 May;25(5):525-9.

6. **Roberts RJ**, Weesner KM, and Bucher JR. Oxygen-induced alterations in lung vascular development in the newborn rat. Pediatr Res. 1983;17: 368–375.

7. **Warner BB**, Stuart LA, Papes RA, and Wispe JR. Functional and pathological effects of prolonged hyperoxia in neonatal mice. Am J Physiol Lung Cell Mol Physiol 1998;275: L110–L117.

8. **Jankov RP**, Luo X, Campbell A, Belcastro R, Cabacungan J, Johnstone L, Frndova H, Lye SJ, Tanswell AK. Fibroblast growth factor receptor-1 and neonatal compensatory lung growth after exposure to 95% oxygen. Am J Respir Crit Care Med 2003;167:1554–1561.

9. **Han RNN**, Buch S, Tseu I, Young J, Christie NA, Frndova H, Lye SJ, Post M, Tanswell AK. Changes in structure, mechanics, and insulinlike growth factor-related gene

expression in the lungs of newborn rats exposed to air or 60% oxygen. Pediatr Res 1996;39:921–929

10. **Yi M**, Jankov RP, Belcastro R, Humes D, Copland I, Shek S, Sweezey NB, Post M, Albertine KH, Auten RL, Tanswell AK. Opposing effects of 60% oxygen and neutrophil influx on alveologenesis in the neonatal rat. Am J Respir Crit Care Med. 2004 Dec 1;170(11):1188-96.

11. **Chang LY**, Subramaniam M, Yoder BA, Day BJ, Ellison MC, Sunday ME, Crapo JD. A catalytic antioxidant attenuates alveolar structural remodeling in bronchopulmonary dysplasia.Am J Respir Crit Care Med. 2003 Jan 1;167(1):57-64

12. **Kinnula VL**, Crapo JD, Raivio KO.Generation and disposal of reactive oxygen metabolites in the lung. Lab Invest. 1995 Jul;73(1):3-19.

13. **Balasubramaniam V**, Mervis CF, Maxey AM, Markham NE, Abman SH. Hyperoxia reduces bone marrow, circulating, and lung endothelial progenitor cells in the developing lung: implications for the pathogenesis of bronchopulmonary dysplasia. Am J Physiol Lung Cell Mol Physiol 2007;292:L1073-L1084.

14. **Abman SH**, Baker C, Balasubramaniam V. Growth and Development of the Lung Circulation: Mechanisms and Clinical Implications. In Bancalari E (ed) The Newborn Lung. Saunders Elsevier, 2008, Philadelphia, pp 50-72.

15. **Jakkula M**, Le Cras TD, Gebb S, Hirth KP, Tuder RM, Voelkel NF, Abman SH. Inhibition of angiogenesis decreases alveolarization in the developing rat lung. Am J Physiol Lung Cell Mol Physiol. 2000 Sep;279(3):L600-7.

16. **Kallapur SG**, Bachurski CJ, Le Cras TD, Joshi SN, Ikegami M, Jobe AH. Vascular changes after intra-amniotic endotoxin in preterm lamb lungs. Am J Physiol Lung Cell Mol Physiol. 2004 Dec;287(6):L1178-85.

17. **Horst SA**, Walther FJ, Poorthuis BJ, Hiemstra PS, Wagenaar GT. Inhaled nitric oxide attenuates pulmonary inflammation and fibrin deposition and prolongs survival in

neonatal hyperoxic lung injury. Am J Physiol Lung Cell Mol Physiol. 2007 Jul;293(1):L35-44.

18. **Lin YJ**, Markham NE, Balasubramaniam V, Tang JR, Maxey A, Kinsella JP, Abman SH. Inhaled nitric oxide enhances distal lung growth after exposure to hyperoxia in neonatal rats. Pediatr Res. 2005 Jul;58(1):22-9.

19. **McCurnin DC**, Pierce RA, Chang LY, Gibson LL, Osborne-Lawrence S, Yoder BA, Kerecman JD, Albertine KH, Winter VT, Coalson JJ, Crapo JD, Grubb PH, Shaul PW. Inhaled NO improves early pulmonary function and modifies lung growth and elastin deposition in a baboon model of neonatal chronic lung disease. Am J Physiol Lung Cell Mol Physiol. 2005 Mar;288(3):L450-9.

20. **Afshar S**, Gibson LL, Yuhanna IS, Sherman TS, Kerecman JD, Grubb PH, et al. Pulmonary NO synthase expression is attenuated in a fetal baboon model of chronic lung disease. Am J Physiol Lung Cell Mol Physiol 2003;284:L749-L758.

21. **Bland RD**, Albertine KH, Carlton DP, MacRitchie AJ. Inhaled nitric oxide effectson lung structure and function in chronically ventilated preterm lambs. Am J Respir CritCare Med 2005;172:899-906.

22. **Murohara T**, Asahara T, Silver M, Bauters C, Masuda H, Kalka C, Kearney M, Chen D, Symes JF, Fishman MC, et al. Nitric oxidesynthase modulates angiogenesis in response to tissue ischemia. J Clin Invest 1998;101:2567–2578.

23. **Zhang R**, Wang L, Zhang L, Chen J, Zhu Z, Zhang Z, Chopp M. Nitric oxide enhances angiogenesis via the synthesis of vascular endothelial growth factor and cGMP after stroke in the rat. Circ Res 2003;92:308– 313.

24. **Kunig AM**, Balasubramaniam V, Markham NE, Morgan D, Montgomery G, Grover TR, Abman SH. Recombinant human VEGF treatment enhances alveolarization after hyperoxic lung injury in neonatal rats. Am J Physiol Lung Cell Mol Physiol 2005;289:L529–L535.

25. **Naseem KM**. The role of nitric oxide in cardiovascular diseases. Mol Aspects Med. 2005 Feb-Apr;26(1-2):33-65.

26. **Bode-Böger SM**, Muke J, Surdacki A, Brabant G, Böger RH,Frölich JC. Oral 1-arginine improves endothelial function in healthy individuals older than 70 years. Vasc Med 2003; 8:77–815.

27. **Piatti PM**, Monti LD, Valsecchi G,Magni F, Setola E, Marchesi F, Galli-Kienle M, Pozza G, Alberti KG. Long-term oral L-arginine administration improves peripheral and hepatic insulin sensitivity in type 2 diabetic patients. Diabetes Care 2001; 24: 875–80.

28. **Walker HA**, McGing E, Fisher I, Böger RH, Bode-Böger SM, Jackson G, Ritter JM, Chowienczyk PJ. Endothelium-dependent vasodilation is independent of the plasma L-arginine/ADMA ratio in men with stable angina: lack of effect of oral L-arginine on endothelial function, oxidative stress and exercise performance. J Am Coll Cardiol 2001; 38: 499–505.

29. **Morris SM Jr**. Enzymes of arginine metabolism. J Nutr. 2004 Oct;134(10 Suppl):2743S-2747S; discussion 2765S-2767S.

30. **Curis E**, Nicolis I, Moinard C, Osowska S, Zerrouk N, Benazeth S, Cynober L. Almost all about citrulline in mammals. Amino Acids 2005; 29: 177–205.

31. **Waugh WH**, Daeschner CW, Files BA,McConnell ME, Strandjord SE. Oral citrulline as arginine precursor may be beneficial in sickle cell disease: early phase two results. J Natl Med Assoc 2001; 93: 363–71.

32. **Chih-Kuang C**, Shuan-Pei L, Shyue-Jye L, Tuan-Jen W. Plasma free amino acids in Taiwan Chinese: the effect of age.Clin Chem Lab Med. 2002 Apr;40(4):378-82

33. **Wu G**. Intestinal mucosal amino acid catabolism. J Nutr. 1998 Aug;128(8):1249-52. Review

34. **Levillain O**, Hus-Citharel A, Morel F, Bankir L. Localization of arginine synthesis along rat nephron. Am J Physiol. 1990 Dec;259(6 Pt 2):F916-23.

35. **Morris CR**, Kuypers FA, Larkin S, Sweeters N, Simon J, Vichinsky EP, Styles LA. Arginine therapy: a novel strategy to induce nitric oxide production in sickle cell disease.Br J Haematol. 2000 Nov;111(2):498-500.

36. **Raghavan SA**, Dikshit M. L-citrulline mediated relaxation in the control and lipopolysaccharide-treated rat aortic rings. Eur J Pharmacol. 2001 Nov 9;431(1):61-9.

37. **Murphy C**, Newsholme P. Importance of glutamine metabolism in murine macrophages and human monocytes to L-arginine biosynthesis and rates of nitrite or urea production. Clin Sci (Lond). 1998 Oct;95(4):397-407.

38. **Hartman WJ**, Torre PM, Prior RL. Dietary citrulline but not ornithine counteracts dietary arginine deficiency in rats by increasing splanchnic release of citrulline. J Nutr. 1994 Oct;124(10):1950-60.

39. **Schwedhelm E**, Maas R, Freese R, Jung D, Lukacs Z, Jambrecina A, Spickler W, Schulze F, Böger RH. Pharmacokinetic and pharmacodynamic properties of oral L-citrulline and L-arginine: impact on nitric oxide metabolism. Br J Clin Pharmacol. 2008 Jan;65(1):51-9.

40. **Vadivel A**, Aschner JL, Rey-Parra GJ, Magarik J, Zeng H, Summar M, Eaton F, Thébaud B. L-Citrulline attenuates arrested alveolar growth and pulmonary hypertension in oxygen-induced lung injury in newborn rats. Pediatr Res. 2010 Aug 27.

41. **Tang K**, Rossiter HB, Wagner PD, Breen EC 2004 Lung-targeted VEGF inactivation leads to an emphysema phenotype in mice. J Appl Physiol 97:1559-1566.

42. **Klekamp JG**, Jarzecka K, and Perkett EA. Exposure to hyperoxia decreases the expression of vascular endothelial growth factor and its receptors in adult rat lungs. Am J Pathol 1999;154: 823–831.

43. **Maniscalco WM**, Watkins RH, Finkelstein JN, and Campbell MH. Vascular endothelial growth factor mRNA increases in alveolar epithelial cells during recovery from oxygen injury. Am J Respir Cell Mol Biol 1995;13:377–386.

44. **Anette M. Kunig**, Vivek Balasubramaniam, Neil E. Markham, Danielle Morgan, Recombinant human VEGF treatment enhances alveolarization after hyperoxiclung injury in neonatal rats, Am J Physiol Lung Cell Mol Physiol 2005, 289: L529–L535, 2005.

45. **Ferrara N**, Gerber HP, and LeCouter J. The biology of VEGF and its receptors. Nat Med 2003;9:669–676.

46. **Grover TR**, Parker TA, Zenge JP, Markham NE, Kinsella JP, and Abman SH. Intrauterine hypertension decreases lung VEGF expression and VEGF inhibition causes pulmonary hypertension in the ovine fetus. Am J Physiol Lung Cell Mol Physiol 2003;284: L508–L517.

47. **Lin**, Tang JR, Markham NE, Lin YJ, McMurtry IF, Maxey A, Kinsella JP, and Abman SH. Inhaled nitric oxide attenuates pulmonary hypertension and improves lung growth in infant rats after neonatal treatment with a VEGF receptor inhibitor. Am J Physiol Lung Cell Mol Physiol 2004;287:L344–L351.

48. **MacRitchie AN**, Albertine KH, Sun J, Lei PS, Jensen SC, Freestone AA, Clair PM, Dahl MJ, Godfrey EA, Carlton DP, and Bland RD. Reduced endothelial nitric oxide synthase in lungs of chronically ventilated preterm lambs. Am J Physiol Lung Cell Mol Physiol 2001;281: L1011–L1020.

49. **Tang**. Afshar S, Gibson LL, Yuhanna IS, Sherman TS, Kerecman JD, Grubb PH, Yoder BA, McCurnin DC, and Shaul PW. Pulmonary NO synthase expression is attenuated in a fetal baboon model of chronic lung disease. Am J Physiol Lung Cell Mol Physiol 2003;284: L749–L758.

50. **Gries DM**, Tam EK, Blaisdell JM, Iwamoto LM, Fujiwara N, Uyehara CF, and Nakamura KT. Differential effects of inhaled nitric oxide and hyperoxia on pulmonary dysfunction in newborn guinea pigs. Am J Physiol Regul Integr Comp Physiol 2000;279: R1525–R1530.

51. **Issa A**, Lappalainen U, Kleinman M, Bry K, and Hallman M. Inhaled nitric oxide decreases hyperoxia-induced surfactant abnormality in preterm rabbits. Pediatr Res 1999;45: 247–254.

52. **McElroy MC**, Wiener-Kronish JP, Miyazaki H, Sawa T, Modelska K, Dobbs LG, and Pittet JF. Nitric oxide attenuates lung endothelial injury caused by sublethal hyperoxia in rats. Am J Physiol Lung Cell Mol Physiol 1997;272: L631–L638.

53. **Brown KR**, England KM, Goss KL, Snyder JM, and Acarregui MJ. VEGF induces airway epithelial cell proliferation in human fetal lung in vitro. Am J Physiol Lung Cell Mol Physiol 2001;281: L1001–L1010.

54. **Chetty C**, Lakka SS, Bhoopathi P, Rao JS. MMP-2 alters VEGF expression via alphaVbeta3 integrin-mediated PI3K/AKT signaling in A549 lung cancer cells. Int J Cancer 2010;127:1081-1095.

55. **Vu TH**, Werb Z. Matrix metalloproteinases: effectors of development and normal physiology. Genes Dev 2000;14:2123–2133.

56. **Crouch E**, Martin G, Brody JS, Laurie G. Basement membranes. In: Crystal RG, West JB, Weibel ER, Barnes PJ (eds) The Lung: Scientific Foundations. Lippincott Raven, Philidelphia, 1997, pp 769–791.

57. **Kheradmand F**, Rishi K, Werb Z. Signaling through the EGF receptor controls lung morphogenesis in part by regulating MT1-MMP-mediated activation of gelatinase A/MMP2. J Cell Sci. 2002 Feb 15;115(Pt 4):839-48.

58. **Danan C**, Jarreau PH, Franco ML, Dassieu G, Grillon C, et al. Gelatinase activities in the airways of premature infants and development of bronchopulmonary dysplasia. Am J Physiol (Lung Cell Mol Biol). 2002;283:L1086–1093.

59. **Schulz CG**, Sawicki G, Lemke RP, Roeten BM, Schulz R, Cheung PY. MMP-2 and MMP-9 and their tissue inhibitors in the plasma of preterm and term neonates. Pediatr Res 2004;55:794–801.

60. **Fukuda Y**, Ishizaki M, Okada Y, Seiki M, Yamanaka N. Matrix metalloproteinases and tissue inhibitor of metalloproteinase-2 in fetal rabbit lung. Am J Physiol Lung Cell Mol Physiol 2000;279:L555–L561.

61. **Itoh T**, Ikeda T, Gomi H, Nakao S, Suzuki T, Itohara S. Unaltered secretion of beta-amyloid precursor protein in gelatinase A (matrix metalloproteinase 2)-deficient mice. J Biol Chem 1997;272:22389–22392.

62. **Fassina G**, Ferrari N, Brigati C, Benelli R, Santi L, Noonan DM, Albini A. Tissue inhibitors of metalloproteases: regulation and biological activities. Clin Exp Metastasis 2000;18:111–120.

63. **Pardo A**, Barrios R, Maldonado V, Melendez J, Perez J, Ruiz V, Segura-Valdez L, Sznajder JI, Selman M. Gelatinases A and B are up-regulated in rat lungs by subacute hyperoxia: pathogenetic implications. Am J Pathol 1998;153:833–844.

64. **Scattoni V**, Montironi R, Mazzucchelli R, Freschi M, Nava L, Losa A, Terrone C, Scarpa RM, Montorsi F, Pappagallo G, Rigatti P. Pathological changes of high-grade prostatic intraepithelial neoplasia and prostate cancer after monotherapy with bicalutamide 150 mg. BJU 2006;Int 98:54-58.

65. **Kubista M**, Andrade JM, Bengtsson M, Forootan A, Jonak J, Lind K, Sindelka R, Sjoback R, Sjogreen B, Strombom L, Stahlberg A, Zoric N. The real-time polymerase chain reaction. Mol Aspects Med 2006;27:95-125.

66. **Masood A**, Yi M, Lau M, Belcastro R, Shek S, Pan J, Kantores C, McNamara PJ, Kavanagh BP, Belik J, Jankov RP, Tanswell AK. Therapeutic effects of hypercapnia on chronic lung injury and vascular remodeling in neonatal rats. Am J Physiol Lung Cell Mol Physiol. 2009 Nov;297(5):L920-30.

67. **Solomonson LP**, Flam BR, Pendleton LC, Goodwin BL, Eichler DC. The caveolar nitric oxide synthase/arginine regeneration system for NO production in endothelial cells. J Exp Biol 2003;206: 2083–2087.

68. **Ananthakrishnan M**, Barr FE, Summar ML, Smith HA, Kaplowitz M, Cunningham G, Magarik J, Zhang Y, Fike CD. L-citrulline ameliorates chronic hypoxia-induced pulmonary hypertension in newborn piglets. Am J Physiol Lung Cell Mol Physiol 2009;297:L506-L511.

69. **Balasubramaniam V**, Ingram DA. Endothelial progenitors in the risk of developing bronchopulmonary dysplasia: can we include endothelial progenitor cells in BPD risk assessment? Am J Respir Crit Care Med 2009;180:488-490.

70. **Ziche M**, Morbidelli L, Choudhuri R, Zhang HT, Donnini S, Granger HJ, Bicknell R. Nitric oxide synthase lies downstream from vascular endothelial growth factor-induced but not basic fibroblast growth factor-induced angiogenesis. J Clin Invest 1997;99:2625-2634.

71. **Dulak J**, Józkowicz A. Regulation of vascular endothelial growth factor synthesis by nitric oxide: facts and controversies. Antioxid Redox Signal 2003;5:123-132.

72. **Crosby LM**, Waters CM. Epithelial repair mechanisms in the lung. Am J Physiol Lung Cell Mol Physiol 2010;298:L715-L731.

73. **Greenlee KJ**, Werb Z, Kheradmand F. Matrix metalloproteinases in lung: multiple, multifarious, and multifaceted. Physiol Rev 2007;87:69-98.

74. **Le NT**, Xue M, Castelnoble LA, Jackson CJ. The dual personalities of matrix metalloproteinases in inflammation. Front Biosci 2007;12:1475-1487.

“La grandezza dell'uomo si misura in base a quel che cerca e all'insistenza con cui egli resta alla ricerca.”

(Heidegger)